

Succession of Ising criticality and its threshold in critical quantum Ising model subject to symmetric decoherence

Yoshihito Kuno,¹ Takahiro Orito,² and Ikuo Ichinose^{3,*}

¹*Graduate School of Engineering science, Akita University, Akita 010-8502, Japan*

²*Department of Physics, College of Humanities and Sciences,*

Nihon University, Sakurajosui, Setagaya, Tokyo 156-8550, Japan

³*Department of Applied Physics, Nagoya Institute of Technology, Nagoya, 466-8555, Japan*

(Dated: August 26, 2025)

We investigate a mixed state quantum criticality in the Ising model under $X + ZZ$ decoherence. In the doubled Hilbert space formalism, the decohered state resides on the self-dual critical line of the quantum Ashkin-Teller (qAT) model, as a result of the specific choice of the decoherence channel. On the other hand, since the mixed state under $X + ZZ$ decoherence satisfies the Kramers-Wannier self-duality in a weak sense, the Ising criticality of the pure state can be partially preserved in the mixed system. By making use of the combination of the doubled Hilbert space formalism and matrix product states, we carry out extensive numerical study to elucidate the mixed state criticality. We find that under decoherence up to moderate strength, the mixed states on the critical line have properties of the Ising CFT, where $c = 1/2$, $\eta = 0.25$ and, $\nu = 1$. These values of the central charge and critical exponents contrast with the ones in the $c = 1$ orbifold boson CFT describing the critical state of the qAT model. In addition, we also observe the threshold of the mixed Ising CFT. The strong decoherence washes out the remnant Ising criticality and induces strong-to-weak spontaneous symmetry breaking.

I. INTRODUCTION

Effects of environment [1, 2] on quantum systems are inevitable. Many-body quantum systems, including ones of great practical use such as quantum computers and quantum memories, are significantly affected by undesired noise and decoherence. Then, the target many-body states are destroyed by noise and/or decoherence when they exceed a threshold [3–6]. However, even if such noise and decoherence change the target state to a mixed state losing the original coherence, some quantum orders of the pure state are to be sustained in the mixed state. For example, the topological order of the toric code [7, 8] is expected to perfectly or partially survive even when the state gets mixed by noise or decoherence, as quantum or sometimes classical memories [9–12]. These examples indicate not only robustness of pure state but also richness of novel mixed states emerging by interactions with environment. That is, effect of noise and decoherence can lead to rich non-trivial quantum mixed states never being created in isolated quantum systems. Noise and decoherence applied to pure quantum states can be an essential ingredient to produce exotic mixed quantum states, which can play an important role in quantum devices.

Along this current research trend, how critical quantum many-body states are affected by various types of decoherence is an on-going issue. We have not completely understood it nor arrived to established consensus. In particular, how decoherence or noise changes physical and information properties of critical states described by conformal field theory (CFT) [13, 14] is an important issue. The fate of the universal property of the well-studied CFTs under decoherence should be investigated in detail.

As a first step toward elucidating this global issue, we study

the simplest pure critical state subject to a specific type of decoherence, that is, the critical ground state of the transverse field Ising model (TFIM) described by Ising CFT [13, 14]. Here, we consider $X + ZZ$ type decoherence. This decoherence has particular properties since the corresponding operation can be regarded as the part of the inter-leg interactions of the quantum Ashkin-Teller (qAT) model in the doubled Hilbert space formalism. Then, the Kraus operators of the decoherence channel possess a Kramers-Wannier (KW) symmetry in a weak sense.

Previous studies [15, 16] have investigated the critical ground state of the transverse field Ising model (TFIM) subject to local Pauli decoherence. It was shown that the CFT subsystem scaling survives. The studies [15, 17] also showed that the universality class of the criticality varies depending on the individual decoherence channel. At present, the mechanism of this nontrivial behavior of critical states under decoherence is poorly understood from universal viewpoint. Building on these prior studies, this work focuses on the TFIM subject to the $X + ZZ$ decoherence, as the resulting mixed state in the doubled Hilbert space formalism is expected to be closely related to the ground states in the qAT model [18–22].

This work numerically clarifies the criticality of the mixed states on the critical line of the phase diagram. In particular, we numerically investigate how the CFT properties of the critical state of the TFIM change or survive under the aforementioned decoherence, with focusing on some physical quantities such as the central charge and critical exponents of correlation functions. Practically, we utilize numerical filtering operation methods applying to the matrix product state (MPS). By this numerical scheme, we calculate the Rényi-2 subsystem entanglement entropy (EE) of mixed states and observe its subsystem dependence in detail.

In general, the Rényi-2 subsystem EE of the mixed state does not agree with that of the pure state [15] since the scaling of the Rényi-2 subsystem EE can exhibit a different form in the leading term of the system size for pure and mixed states.

* A professor emeritus

But it has the same CFT scaling form for the subleading term in both states. Thus, we focus on the subscaling term in the decohered system. According to Ref. [15], the scaling form of the subleading term can be elucidated by introducing the Rényi-2 mutual information composed of the Rényi-2 subsystem EE. Its scaling form obeys the CFT scaling of Rényi-2 mutual information given as,

$$\frac{c_2}{4} \ln \left[\frac{L}{\pi} \sin \left(\frac{\ell\pi}{L} \right) \right] + \gamma,$$

where L is the system size (we employ periodic boundary conditions), ℓ is subsystem size, c_2 is Rényi-2 central charge, and γ is non-universal constant. In particular, there exists a conjecture [23–27]; $c_2 = 2c_{\text{eff}}$, where c_{eff} is an effective central charge, and for Ising CFT states, $c_{\text{eff}} = 1/2$, that is, the central charge of the Ising CFT [13]. This conjecture has been numerically tested in the projective measurement limit of the critical state of the TFIM [24–27], to find the robustness of the CFT scaling and the central charge. However, this robustness of the CFT properties under decoherence has been observed for particular cases and there is no rigorous proof even for some specific cases. Thus, further numerical investigation is desired.

Through the known phase diagram of the qAT model, the phase diagram of the target decohered state can be inferred, and actually the previous work [28] confirmed the presence of various mixed state phases; counterparts of those in the qAT model. But the criticality has not been elucidated in detail. In this work, we investigate how the criticality of the TFIM evolves under $X + ZZ$ decoherence by observing the Rényi-2 subsystem EE, etc. In our decoherence setup, furthermore, the weak KW self-duality is kept. This gives an expectation of the survival of the Ising CFT. Through the extensive numerics, we verify that the mixed states on the phase boundary line preserve the genuine critical properties of the pure Ising CFT for the symmetric decoherence up to some moderate strength, contrary to the expectation from the qAT picture indicating the orbifold boson CFT. Further, we observe the threshold of the CFT property and show the emergence of the Z2 strong-to-weak spontaneous symmetry breaking (SWSSB) phase.

The rest of this paper is organized as follows. In Sec. II, we explain the setting of the system in this work and consider effects of the $X + ZZ$ decoherence and qualitative relationship to the qAT model. In Sec. III, we introduce quantum entanglement measures and some physical quantities to evaluate the criticality of the mixed state. Then, efficient numerical calculation methods are reviewed, where we introduce the doubled Hilbert space formalism. In Sec. IV, we display results of numerical calculations by using the MPS and the filtering to the MPS for various decoherence parameters. Section V is devoted to conclusion and discussion.

Here, we give an important comment on the reliability of the doubled Hilbert space formalism. We employ this formalism for numerical calculation to evaluate the criticality of the mixed states. However up to date, study demonstrating that exponents obtained by the doubled Hilbert space formalism for decohered mixed states agree with rigorous critical exponents is lacking. We proceed with numerical calculations

on the standpoint that the formalism is reliable and gives correct results. In trivial cases, we have carefully confirmed that the criticality obtained by the doubled formalism agrees with that obtained rigorously. Thus, the numerical calculations that we shall present in the doubled Hilbert space formalism give valuable results to the ends of this work. Rigorous proof of the correctness of quantitative results by the doubled-Hilbert space formalism is beyond the scope of the present study.

II. TARGET SYSTEM UNDER DECOHERENCE

A. Model and decoherence

This work studies the 1D TFIM, the Hamiltonian of which is given by,

$$H_0 = - \sum_{j=0}^{L-1} [JZ_j Z_{j+1} + hX_j],$$

where J and h are model parameters and periodic boundary conditions (PBCs) are imposed. The system possesses Z_2 symmetry, the generator of which is a global spin flip $\prod_{j=0}^{L-1} X_j$. At $J = h$, a critical ground state appears and is described by the Ising CFT[13, 14]. For $J/h > 1$, the ground state is Z_2 SSB ferromagnetic (FM) and for $J/h < 1$, a paramagnetic (PM) state emerges. Hereafter, we denote the ground state of H_0 by $|\psi_0\rangle$, and its (pure-state) density matrix by $\rho_0 = |\psi_0\rangle\langle\psi_0|$, and \mathcal{H} is the Hilbert space of the spin-1/2 L -site system.

In this work, we consider two types of the tunable decoherence channels given as [29]

$$\begin{aligned} \mathcal{E}_{ZZ}[\rho] &= \prod_{j=0}^{L-1} \mathcal{E}_{ZZ,j}[\rho], \\ \mathcal{E}_{ZZ,j}[\rho] &= \left[(1 - p_{zz})\rho + p_{zz}Z_j Z_{j+1}\rho Z_{j+1}Z_j \right], \\ \mathcal{E}_X[\rho] &= \prod_{j=0}^{L-1} \mathcal{E}_{X,j}[\rho], \\ \mathcal{E}_{X,j}[\rho] &= \left[(1 - p_x)\rho + p_x X_j \rho X_j \right], \end{aligned}$$

where $p_{zz(x)}$ is the strength of the decoherence and $0 \leq p_{zz(x)} \leq 1/2$. The two types of decoherence are uniformly applied to the whole system as [30]

$$\rho_D \equiv \mathcal{E}_{ZZ} \circ \mathcal{E}_X[\rho_0].$$

In the previous work of the present authors [28], the phase diagram of the mixed state ρ_D is clarified as in Fig. 1, in which there exist three phases, mixed FM, mixed PM, and SWSSB phase [28]. There, phase boundaries were obtained by studying spin correlation functions and entanglement of the doubled system in the doubled Hilbert space formalism. More detailed are explained in the following subsection after introducing the doubled Hilbert space formalism.

The aim of this work is to clarify the behavior of the state on the phase boundary between the mixed FM and mixed PM. The combination of the two decoherences \mathcal{E}_{ZZ} and \mathcal{E}_X under the conditions, $J = h$ and $p_{zz} = p_x$ becomes the following form

$$\mathcal{E}_D[\rho] = \prod_{j=0}^{L-1} \mathcal{E}_D^j[\rho], \quad (1)$$

$$\mathcal{E}_D^j[\rho] = \sum_{\ell=0,1,2,3} K_j^\ell \rho K_j^{\ell,\dagger}, \quad (2)$$

where $K_j^{\ell=0,1,2,3}$ is a Kraus operator given by $K_j^0 = (1 - p_D)I$, $K_j^1 = \sqrt{p_D(1 - p_D)}X_j$, $K_j^2 = \sqrt{p_D(1 - p_D)}Z_j Z_{j+1}$ and $K_j^3 = p_D X_j Z_j Z_{j+1}$ with a condition $\sum_{\ell} K_j^\ell K_j^{\ell,\dagger} = I$, $p_D \equiv p_{zz(x)}$ and the strength of the decoherence is tuned by p_D , taking $0 \leq p_D \leq 1/2$. For $p_D = 1/2$, these channels correspond to projective measurements of $Z_j Z_{j+1}$ and X_j without monitoring and are called maximal decoherence. It is easily verified that the decoherence \mathcal{E}_D is weakly symmetric under the KW transformation, $Z_j Z_{j+1} \rightarrow X_j$ and $X_j \rightarrow Z_j Z_{j+1}$ if we ignore rigorous consideration to boundary constraints [31]. In fact, each K_j^α is transformed to its pair Kraus operator under the KW transformation showing weak symmetry of the decoherence channel [32, 33].

B. Doubled Hilbert space formalism and qualitative connection to quantum Ashkin-Teller model

The qualitative phase structure of the decohered state ρ_D can be understood from the doubled Hilbert space formalism of the present system. We briefly review this formalism and show that the mixed phase diagram can be over-viewed from the qAT model [19, 34].

To explain the doubled Hilbert space formalism, we consider a state in a Hilbert space, $\rho \in \mathcal{H}$. In the doubled Hilbert space formalism, the target Hilbert space is doubled as $\mathcal{H}_u \otimes \mathcal{H}_\ell$, where the subscripts u and ℓ denote the upper and lower Hilbert spaces corresponding to ket and bra states of mixed state density matrix, respectively. A density matrix ρ can be vectorized $\rho \rightarrow |\rho\rangle\rangle$ [35, 36] as $|\rho\rangle\rangle \equiv \frac{1}{\sqrt{\dim[\rho]}} \sum_k |k\rangle \otimes \rho |k\rangle$, where $\{|k\rangle\}$ is an orthonormal set of bases in the Hilbert space \mathcal{H} . Then, the state $|\rho\rangle\rangle$ is in the doubled Hilbert space $\mathcal{H}_u \otimes \mathcal{H}_\ell$.

In this formalism, decoherence channels can be mapped into an operator acting on the vector $|\rho\rangle\rangle$ [37, 38]. Concretely, the Kraus operator sum of a decoherence represented by $\mathcal{E}[\rho] = \sum_{\alpha=0}^{M-1} K_\alpha \rho K_\alpha^\dagger$, where K_α 's are Kraus operators, is turned into an operator in the space $\mathcal{H}_u \otimes \mathcal{H}_\ell$, given by $\hat{\mathcal{E}} = \sum_{\alpha=0}^{M-1} K_{\alpha,u}^* \otimes K_{\alpha,\ell}$. The action of the decoherence is performed as $\hat{\mathcal{E}}|\rho\rangle\rangle$, which is a decohered state in the doubled Hilbert space.

We consider the target system from the view of the doubled Hilbert space formalism. We set the input density matrix ρ_0 to be the ground state of the TFIM, denoted by $|\rho_0\rangle\rangle \equiv |\psi_0^*\rangle |\psi_0\rangle$.

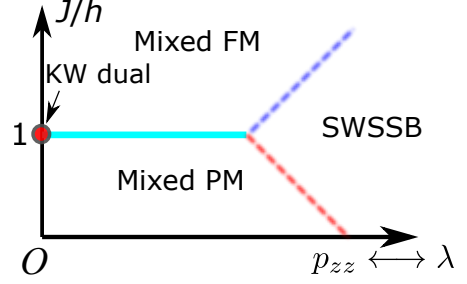


FIG. 1. Schematic phase diagram of mixed states. The existence of each mixed phase has been clarified in the previous work [28]. In our numerical calculation, the strength of decoherence, p_{zz} and p_x is related to λ in the qAT model as $\lambda \leftrightarrow \tanh^{-1}[p_{zz(x)}/(1 - p_{zz(x)})]$ with the constraint $p_x = 1/2 - (1/2)(1 - 2p_{zz})^{1/J}$. The global mixed phase diagram of the doubled system is closely related to that of the qAT model [18]. The right blue line is a critical phase boundary line expected in [28]. The red point is the KW duality point of the TFIM.

The state $|\rho_0\rangle\rangle$ can be regarded as two copies of the ground state of the 1D TFIM $|\psi_0\rangle$, whereas the asterisk denotes the complex conjugation. The doubled system then is a two-decoupled TFIM on a two-leg spin-1/2 ladder based on the doubled Hilbert space $\mathcal{H}_u \otimes \mathcal{H}_\ell$.

Next, in this formalism, the decoherence channel $\mathcal{E}_{ZZ} \circ \mathcal{E}_X$ acting on $|\rho_0\rangle\rangle$ can be treated as a filtering operator $\hat{\mathcal{E}}_{ZZ} \hat{\mathcal{E}}_X$. The decohered state is given by

$$|\rho_D\rangle\rangle \equiv \hat{\mathcal{E}}_{ZZ} \hat{\mathcal{E}}_X |\rho_0\rangle\rangle \propto \prod_{j=0}^{L-1} \left[e^{\tau_{zz} \hat{h}_{j,j+1}^{zz}} e^{\tau_x \hat{h}_j^x} \right] |\rho_0\rangle\rangle, \quad (3)$$

where $\hat{h}_{j,j+1}^{zz} = Z_{j,u} Z_{j+1,u} \otimes Z_{j,\ell} Z_{j+1,\ell}$, $\hat{h}_j^x = X_{j,u} \otimes X_{j,\ell}$, $\tau_{zz(x)} = \tanh^{-1}[p_{zz(x)}/(1 - p_{zz(x)})]$. In general, the state $|\rho_D\rangle\rangle$ is not a normalized state [39]. Equation (3) can be viewed that the state $|\rho_0\rangle\rangle$ is locally-filtered by the two different kinds of local perturbative operators $e^{\tau_{zz} \hat{h}_{j,j+1}^{zz}}$ and $e^{\tau_x \hat{h}_j^x}$, which is analogue to the imaginary time evolution emerging the state $|\rho_D\rangle\rangle$ [40–43].

Based on the previous studies [42–45], this perturbative picture of the decoherence operation gives an effective Hamiltonian picture in the doubled system regarded as the spin-1/2 ladder system. The decoherence operation adds effective interactions to the doubled TFIM Hamiltonian of the ladder system. Then, we expect that the decohered state is qualitatively close to the ground state of the TFIM Hamiltonian with the effective interactions [46], where the strengths of the effective interaction are proportional to τ_{zz} and τ_x tuned by p_{zz} and p_x . The effective Hamiltonian of which is given on the ladder as

the qAT model [18],

$$H_{qAT} = -J \sum_{j=0}^{L-1} [Z_{j,u} Z_{j+1,u} + Z_{j,\ell} Z_{j+1,\ell} + \lambda_{zz} Z_{j,u} Z_{j,\ell} Z_{j+1,u} Z_{j+1,\ell}] - h \sum_{j=0}^{L-1} [X_{j,u} + X_{j,\ell} + \lambda_x X_{j,u} X_{j,\ell}].$$

The global ground state phase diagram of H_{qAT} has been already investigated in detail [18, 21, 22]. There are three representative ground-state phases for the region $\lambda_{zz} = \lambda_x \equiv \lambda > 0$ (since $\tau_{zz(x)} > 0$) [18, 20]: Phase I. Double chain spontaneous Z_2 symmetry broken phase, Phase II Double paramagnetic phase. Phase III. Diagonal Z_2 symmetric phase (also called “partially-ordered phase”).

The previous study of the authors [28] clarified that the decohered state $|\rho_D\rangle\rangle$ exhibits three mixed phases related to the above three phases in the qAT model: The phases I, II and III correspond to mixed FM phase, mixed PM and SWSSB phases, respectively. A schematic phase diagram is shown in Fig. 1. Phase boundary between the phases I and II is obtained by the standard spin-spin correlation function, whereas the phase III can be recognized by the spin-spin correlation function in the doubled Hilbert space (see later discussion). The EE also exhibits anomalous behavior indicating transitions between the three phases. However, the detailed knowledge of the criticality of the mixed system is still lacking, and therefore, we shall study it in detail in this work.

For the qAT model, the criticality of the phase boundary $J/h = 1$ was numerically investigated in detail [22] (pure state framework). The λ -term in H_{qAT} is a marginal perturbation, inducing a continuous change of the criticality, the image of which is shown by the right-blue line in Fig. 1. The criticality holds on the line, $-1/\sqrt{2} \leq \lambda \leq 1$ and is described by the orbifold boson CFT [47].

Here, a question arises if the orbifold boson CFT of the qAT model is an effective field theory for the critical state under the $X + ZZ$ decoherence. In other words, we would like to elucidate how the criticality of the system changes under decoherence, as we explained in introduction. In what follows, we study this issue by investigating the subsystem Rényi-2 entanglement entropy and correlation functions on the critical line.

III. PHYSICAL OBSERVABLES

To elucidate the criticality of the mixed state, we introduce some physical quantities. The first one is the subsystem Rényi-2 mutual information, the Rényi-2 mutual information (R2MI) defined as,

$$MI^{(2)}(L_A) \equiv S_A^{(2)} + S_B^{(2)} - S_{A \cup B}^{(2)}, \quad (4)$$

where the system divided into two halves, denoted by the subsystem A and B and $A \cup B$ represents the entire system. L_A

is the subsystem size of the subsystem A . Here, $S_X^{(2)}$ is defined as $S_X^{(2)} = -\log \text{Tr}[\rho_{D,X}^2]$ where $\rho_{D,X} \equiv \text{Tr}_{\bar{X}}[\rho_D^2]$. The practical calculation scheme in the doubled Hilbert space formalism has been developed [48] as briefly explained in Appendix A.

The second and third observables are the (reduced) susceptibilities of the Rényi-2 ZZ and conventional ZZ correlators,

$$\chi^{\text{II}} = \frac{2}{L} \sum_{r=1}^{L/2} C_{ZZ}^{\text{II}}(0, r), \quad (5)$$

$$\chi^{\text{I}} = \frac{2}{L} \sum_{r=1}^{L/2} C_Z^{\text{I}}(0, r). \quad (6)$$

Here,

$$C_{ZZ}^{\text{II}}(i, j) \equiv \frac{\langle\langle \rho_D | Z_{i,u} Z_{j,u} Z_{i,\ell} Z_{j,\ell} | \rho_D \rangle\rangle}{\langle\langle \rho_D | \rho_D \rangle\rangle},$$

$$C_Z^{\text{I}}(i, j) \equiv \frac{\langle\langle \mathbf{1} | Z_{i,u} Z_{j,u} | \rho_D \rangle\rangle}{\langle\langle \mathbf{1} | \rho_D \rangle\rangle}. \quad (7)$$

where $|\mathbf{1}\rangle\rangle \equiv \frac{1}{2^{3L/2}} \prod_{j=0}^{L-1} |t\rangle_j$ with $|t\rangle_j = |\uparrow_u \uparrow_\ell\rangle_j + |\downarrow_u \downarrow_\ell\rangle_j$.

In the original physical 1D system, $C_{ZZ}^{\text{II}}(i, j)$ corresponds to the Rényi-2 correlator; $C_{ZZ}^{\text{II}}(i, j) \equiv \frac{\text{Tr}[Z_i Z_j \rho_D Z_i Z_j \rho_D]}{\text{Tr}[(\rho_D)^2]}$, identifying the spontaneous symmetry breaking (SSB) of strong symmetry but *not* that of the weak one [37, 49, 50]. $C_{ZZ}^{\text{II}}(i, j) \neq 0$ for $|i - j| \rightarrow \infty$ indicates the emergence of a SSB state. $C_Z^{\text{I}}(i, j)$ in the original physical Hilbert space is given by $\text{Tr}[\rho_D Z_i Z_j]$, which is the canonical two point ZZ correlation, diagnosing the weak SSB. The more explanation about $C_Z^{\text{I}}(i, j)$ is given in Appendix B. The quantities χ^{II} and χ^{I} are used as order parameters of these SSB's. The combination of χ^{II} and χ^{I} can detect the SWSSB, which is recently proposed in Refs. [28, 37, 49, 50] for strong symmetric systems. In the doubled Hilbert space formalism, a state with $\chi^{\text{II}} \sim \mathcal{O}(1)$ and $\chi^{\text{I}} \sim 0$ exhibits SSB of the off-diagonal (i.e., strong) symmetry and also the restoration of the diagonal (i.e., weak) symmetry [37].

Here, we comment on weak KW self-duality in order. A weak KW self-dual density matrix ρ satisfies the following equation,

$$(KW)\rho(KW) = \rho,$$

where (KW) schematically stands for the KW transformation. It is easily verified that the relation between the Rényi-2 correlations diagnoses if the state has the weak KW symmetry;

$$\text{Tr}[Z_i Z_j \rho Z_j Z_i \rho] = \text{Tr}\left[\left(\prod_{i \leq \ell < j} X_\ell\right) \rho \left(\prod_{i \leq \ell < j} X_\ell\right) \rho\right], \quad (8)$$

where the quantity on the RHS is nothing but the disorder parameter of weak Z_2 symmetry. If the above equality holds, the state keeps the weak KW symmetry. We numerically verified

the above equality for the states on the line $J = h$ and for a finite p_{zz} regime. (See Appendix C). This fact implies that the critical mixed states with the weak KW duality can possess the properties of the Ising CFT since as a broad consensus the pure critical state with the KW duality in the TFIM possesses the properties of the Ising CFT.

IV. NUMERICAL INVESTIGATION

In this section, we numerically investigate states on the phase boundary line between the mixed PM and FM phases. The parameter sweep is performed by varying p_{zz} with $p_x = 1/2 - (1/2)(1 - 2p_{zz})^{1/J}$. In most cases, we focus on the case $J = h = 1$.

We generate the decohered state $|\rho_D\rangle\rangle$ by using the MPS formalism, which can analyze large ladder systems and clarify subsystem entanglement of the decohered state $|\rho_D\rangle\rangle$. For the numerical treatment of the MPS, we employ the TeNPy library [51, 52].

First, we prepare the initial state $|\rho_0\rangle\rangle$, which is the ground state of the decoupled 1D TFIM on the ladder by the density matrix renormalization group algorithm. Then, the decoherence operation [the filtering operation in Eq. (3)] $\hat{E}_{ZZ}\hat{E}_X|\rho_0\rangle\rangle$ is efficiently carried out by the TeNPy package.

In all the following numerical simulations, we treat the MPS with maximum bond dimension $D = 300$, where singular values less than $\mathcal{O}(10^{-6})$ are truncated. In the density matrix renormalization group algorithm, the energy convergence of the iterative sweeping is $\Delta E < \mathcal{O}(10^{-5})$ to obtain the initial MPS ground state. We then obtain the state $|\rho_D\rangle\rangle = \hat{E}_{ZZ}\hat{E}_X|\rho_0\rangle\rangle$ for various values of p_{zz} .

A. Subsystem Rényi-2 mutual information

We observe the subsystem Rényi-2 mutual information. As the previous works [15, 53] showed, the subsystem Rényi-2 EE exhibit the following scaling form if the system is described by a CFT

$$S_A^{(2)}(L_A) = \alpha_0 L_A + \frac{c_{\text{eff}}}{4} \log \left[\frac{L}{\pi} \sin \left(\frac{\pi L_A}{L} \right) \right] + \alpha_1. \quad (9)$$

The subsystem EE has an extensive term proportional to L_A , but the sub-leading sine function term is universal, and c_{eff} is called an effective central charge whereas the coefficient α_0 is nonuniversal. As the above scaling form has not been derived analytically in our system, we shall numerically investigate the presence of the sub-leading term to confirm the scaling law (9) and extract the effective central charge. In the following, we numerically examine if the R2MI satisfies the scaling law derived from Eq. (9) [15],

$$MI^{(2)}(L_A) = \frac{c_{\text{eff}}}{2} \log \left[\frac{L}{\pi} \sin \left(\frac{\pi L_A}{L} \right) \right] + \beta_1, \quad (10)$$

where β_1 is a non-universal constant. The reason why we use the R2MI instead of the EE is that c_{eff} can be precisely

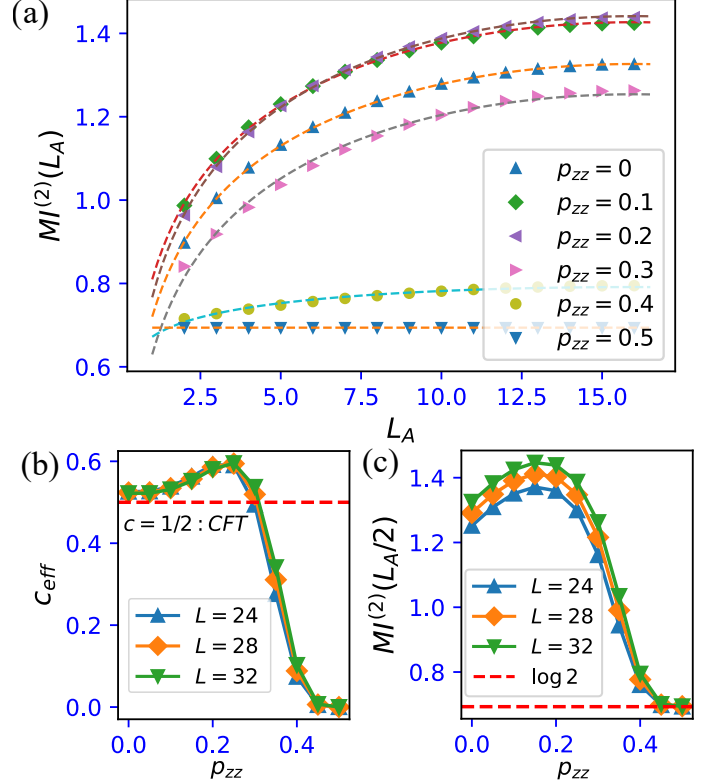


FIG. 2. (a) Subsystem size dependence of R2MI for various p_{zz} 's. We set $L = 28$. (c) p_{zz} -dependence effective extracted central charge for different system sizes. (b) p_{zz} -dependence of R2MI for $L_A = L/2$. For all data, we set $J = h = 1$.

estimated by the numerical optimization procedure, eliminating the non-universal extensive term with the coefficient α_0 in $S_A^{(2)}(L_A)$ [Eq. (9)].

Figure 2 (a) shows numerical results of the L_A dependence of the R2MI for various values of p_{zz} . We find that the clear CFT scaling (sine function form) appears up to $p_{zz} = 0.3$ and for $p_{zz} \gtrsim 0.4$, the sine function form of the CFT scaling is suppressed. It is understood that Ising CFT criticality survives up to $p_{zz} = 0.3$ even under the $X + ZZ$ decoherence applied to the pure Ising critical ground state. Then, there is a drastic change between $p_{zz} = 0.3$ and $p_{zz} = 0.4$ data, indicating the drastic change of the mixed state.

In order to clarify the CFT criticality, we numerically evaluate the effective central charge c_{eff} from the data shown in Fig. 2(b). We confirmed that at $p_{zz} = 0$ (without the decoherence) $c_{\text{eff}} \sim 1/2$ consistent to the central charge of the Ising CFT based on the expectation for the Rényi-2 EE [23–27]. Then we find that for moderate values of p_{zz} , the data are significantly close to $1/2$. This implies that the central charge of the Ising criticality of the pure critical ground state of the TFIM continuously keeps even as switching on the decoherence. The mixed state criticality between the mixed FM and PM is different from that of the compact boson CFT ($c = 1$)

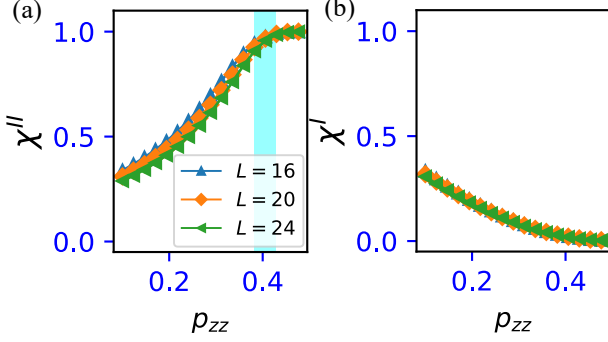


FIG. 3. p_{zz} -dependence of χ_{ZZ}^{II} [(a)] and χ^I [(b)]. From the right-blue regime in (a), the system size dependence vanishes and the values are saturated to almost unity.

well-verified in the qAT model[22, 54]. Thus, we claim that for the mixed case, the existence of the phase boundary is the same with the qAT model, but the criticality is different in the two systems.

For $p_{zz} > 0.3$, the extracted value of c_{eff} deviates from $1/2$ and suddenly drops. For $p_{zz} > 0.4$, the value vanishes. This indicates that the surviving Ising CFT disappears and a different mixed state appears. Along with the behavior, we further plot the R2MI for $L_A = L/2$ in Fig. 2(c). The finite values of $MI^{(2)}(L_A)$ with a system size dependence for $0 \leq p_{zz} \leq 0.3$ appears. For $p_{zz} \gtrsim 0.3$, the value exhibits a sudden drop and settles down a constant value $\ln 2$. That is, for large p_{zz} regime, the mixed state has a finite correlation.

As the central charge measures how many gapless states exist in the system, this drastic change in the behavior of c_{eff} and R2MI indicates that some kind of gap-opening mechanism starts to work by decoherence and the system loses gapless modes although it is difficult to define the gap in the mixed state [55]. As discussed in the previous study [28], decoherence strong enough induces SWSSB of the Z_2 symmetry, and we think that this drastic change of c_{eff} and R2MI is a kind of its “primordial” phenomenon. The threshold of the Ising CFT can correspond to the emergence of the SWSSB. Therefore, the changes in the strong decoherence regime should be discussed through the Rényi-2 ZZ correlation as we do in the next section.

B. Rényi-2 ZZ correlator

To elucidate the behavior of the R2MI and its corresponding CFT, we here observe the susceptibilities for Rényi-2 ZZ correlator, χ^I and χ^{II} . These observables can characterize the emergence of the Z_2 SWSSB [49] and are numerically tractable. These have already been observed in our previous study [28]. In this work, we reproduce the results in the precise numerical conditions [especially, bond dimension $D = 300$, etc.].

The reproduced results are shown in Fig. 3 (a) and (b). In

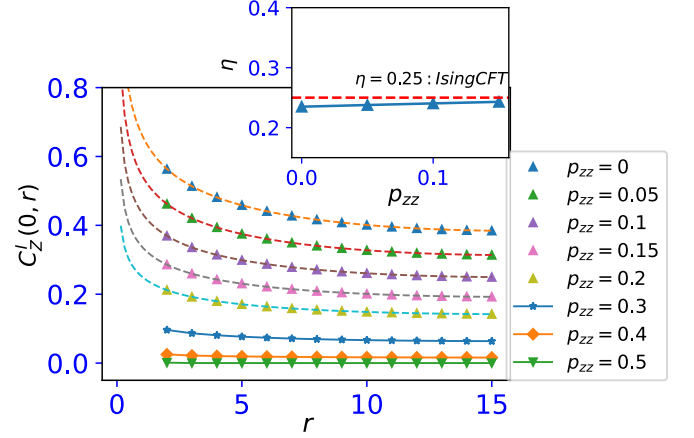


FIG. 4. Behavior of the correlation function $C_Z^I(0, r)$. Data of $p_{zz} = 0.05, 0.1, 0.15, 0.2$ are well-fitted by the power-law decay, while the other data, $p_{zz} = 0.3, 0.4$ and 0.5 , are not. Inset: Numerically extracted η from the ansatz of Eq.(13). We set $J = h = 1$. The data are obtained for the $L = 32$ system.

the regime $p_{zz} > 0.4$, the SWSSB takes place, and as we observed in the above, the effective central charge c_{eff} vanishes. This fact indicates that the SWSSB of the Z_2 symmetry in the system substantially eliminates the Ising CFT properties. The threshold of the Ising CFT in the mixed system is just right before the onset of the SWSSB.

C. Canonical ZZ and XX correlation functions

In addition to the observation of the central charge in the preceding subsection, we shall show further evidences for the possible Ising critical properties of the mixed state under the decoherence.

We observe the behavior of the canonical ZZ correlation function defined by Eq. (7). If the Ising CFT succeeds up to moderate-strength decoherence, the canonical ZZ correlation function exhibits the property of the Ising CFT. In particular, the Ising CFT has the following form of the ZZ correlation function,

$$C_Z^I(0, r) = \gamma_0 \left(\frac{\pi}{L \sin(\pi r/L)} \right)^\eta, \quad (11)$$

where the appearance of the sine function respects the chord distance r due to the PBC. This sine-function part reflects the power law decay of the correlation, and η is the conventional critical exponent of the spin correlation function.

Figure 4 displays the r -dependence of $C_Z^I(0, r)$ for typical p_{zz} 's. The mixed states on the phase boundary ($p_{zz} = 0.05, 0.1, 0.15, 0.2$ data) clearly exhibit the power-law decay, while the other data, $p_{zz} = 0.3, 0.4$ and 0.5 (SWSSB regime) do not. Then, we extract the value of η through the ansatz with Eq. (11). The result is shown in the inset of Fig. 4. We find the values of η on the phase boundary line are very close to the

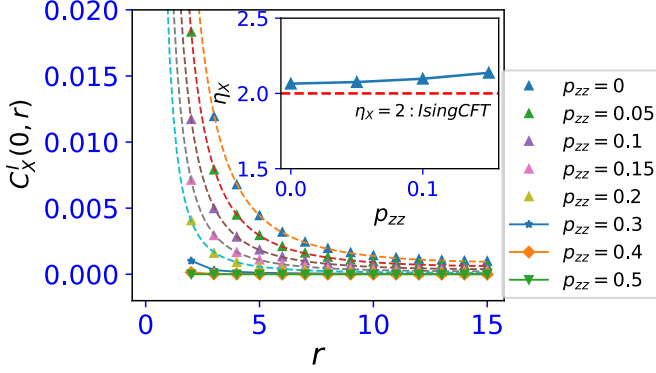


FIG. 5. Behavior of the correlation function $C_X^I(0, r)$. Data of $p_{zz} = 0.05, 0.1, 0.15$ and 0.2 are well-fitted by the power-law decay, while the other data, $p_{zz} = 0.3, 0.4$ and 0.5 , are not. Inset: Numerically extracted η from the ansatz of Eq.(13). We set $J = h = 1$. System size $L = 32$.

one of the Ising CFT, 0.25 . In passing, we also comment that γ_0 in Eq. (11) is a decreasing function of p_{zz} , and this makes χ^I in Fig. 3(b) a decreasing function of p_{zz} .

Here, we note that the behavior of the ZZ spin correlation function on the critical line of the qAT model. The value of η has been exactly obtained as $\eta = 1/4$, and therefore, we cannot judge whether the above critical property of the decohered mixed state stems from the Ising or the qAT criticality.

Then, we further study its criticality by investigating the XX correlation function, for which the Ising and qAT models exhibit different behavior. Here, we introduce the canonical connected XX correlation function defined similarly to the ZZ correlation function in Eq. (7),

$$C_X^I(i, j) \equiv \frac{\langle \langle \mathbf{1} | X_{i,u} X_{j,u} | \rho_D \rangle \rangle}{\langle \langle \mathbf{1} | \rho_D \rangle \rangle} - \frac{\langle \langle \mathbf{1} | X_{i,u} | \rho_D \rangle \rangle \langle \langle \mathbf{1} | X_{j,u} | \rho_D \rangle \rangle}{\langle \langle \mathbf{1} | \rho_D \rangle \rangle \langle \langle \mathbf{1} | \rho_D \rangle \rangle}. \quad (12)$$

As the ZZ correlation function, it is expected to obey the following form predicted by the CFT,

$$C_X^I(0, r) = \gamma_0^X \left(\frac{\pi}{L \sin(\pi r/L)} \right)^{\eta_X}. \quad (13)$$

This sine-function part reflects the power law decay of the correlation and η_X is the critical exponent. For the pure Ising critical state, it has been obtained that $\eta_X = 2$, whereas for the qAT model, the value of η_X is λ -dependent and given by $\eta_X = \pi / \arccos(-\lambda)$, a decreasing function of positive λ and then p_{zz} .

The numerical results are shown in Fig. 5. Up to a moderate p_{zz} , $C_X^I(0, r)$ clearly exhibits a power-law decay, and we extract η_X and plot them in the inset in Fig. 5. The results indicate that, up to a moderate p_{zz} , the extracted values of η_X are close to 2 . It clearly provides a strong evidence to us that the decohered mixed state belongs to the Ising CFT universality class.

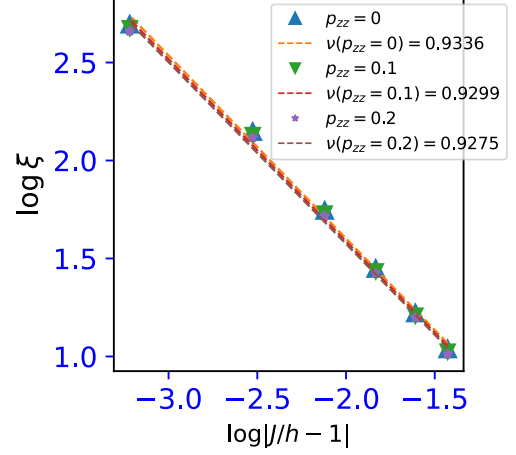


FIG. 6. Log-log plot for correlation length. The data of $C_Z^I(0, r)$ are calculated for $L = 28$ system.

We further verify whether the phase boundary line between the mixed FM and PM exhibits the properties of the Ising CFT. To obtain another evidence for that, we observe the behavior of the canonical ZZ correlation function as varying J in the TFIM with $h = 1$, p_{zz} fixed and $p_x = p_x = 1/2 - (1/2)(1 - 2p_{zz})^{1/J}$. This parameter sweep corresponds to orthogonally moving to the phase boundary line. Under this sweep, we calculate $C_Z^I(0, r)$ for various J with L fixed. Here, we expect that near the phase boundary, $C_Z^I(0, r)$ exhibits the following exponential decay,

$$C_Z^I(0, r) = a_0 \exp \left[-\frac{r}{\xi(J/h)} \right] + a_1, \quad (14)$$

where a_0 and a_1 are non-universal constant and $\xi(J/h)$ is a correlation length depending on J/h . From the correlation length $\xi(J/h)$, we here define the correlation length critical exponent ν as $\xi(J/h) \propto |J/h - 1|^\nu$.

We estimate the correlation length $\xi(J/h)$ by fitting the data of $C_Z^I(0, r)$ to the form Eq.(14). Figure 6 shows the log-log plot of the extracted $\xi(J/h)$ vs $|J/h - 1|$. We then carry out the fitting $\xi(J/h) \propto |J/h - 1|^\nu$ for the data and estimate the value of ν . We find that the extracted value ν for $p_{zz} \leq 0.2$ is close to 1 as shown in Fig. 6, independently to the value of p_{zz} . This means that the exponent is different from that of the qAT model (orbifold boson CFT), in which $\nu = 1/[2 - (\pi/2)(\arccos(-\lambda))^{-1}]$ [18]. In the Ising CFT, the exact correlation length critical exponent is $\nu = 1$ [13]. Thus, the obtained result for the exponent ν is another evidence for the Ising CFT critical behavior of the mixed state under consideration.

These numerically obtained facts conclude that the mixed phase boundary line retains characteristics of the Ising CFT.

V. SUMMARY AND CONCLUSION

We investigated the fate of the Ising CFT on the critical Ising model under the $X + ZZ$ decoherence by employing the efficient numerical scheme based on the doubled Hilbert space formalism. In the effective Hamiltonian picture, the decohered state is expected to possess a critical phase boundary up to a large decoherence regime. In the pure state picture by the qAT model, the boundary line is the orbifold boson CFT [18, 21]. On the other hand, the weak KW duality is respected in the target mixed system, and then, we expect that the pure Ising CFT can be preserved.

Our numerics indicates that the criticality of the mixed state phase boundary has a remaining Ising CFT. The subsystem dependency of the R2MI exhibits CFT scaling, where the numerically extracted central charge is substantially close to Ising CFT $c = 1/2$. Moreover, the critical exponents numerically extracted support the remaining Ising CFT even in the mixed state.

We further investigate the threshold of the mixed criticality up to large decoherence strength. From the behavior of the central charge numerically extracted by the CFT scaling ansatz, the central charge suddenly vanishes around $p_{zz} \sim 0.4$, indicating the mixed state Ising CFT is swept out and the critical mixed state is no longer stable. Then, the SWSSB characterized by Rényi-2 ZZ correlation supports the above behavior of the system. That is, vanishing the remaining Ising CFT corresponds to the appearance of the SWSSB.

ACKNOWLEDGEMENTS

This work is supported by JSPS KAKENHI: JP23K13026(Y.K.) and JP23KJ0360(T.O.).

DATA AVAILABILITY

The data that support the findings of this study are available from the authors upon reasonable request.

APPENDIX

Appendix A: Calculation scheme for subsystem Rényi-2 entanglement entropy

We show a calculation scheme for the subsystem Rényi-2 EE, where the subsystem is X . The process of the partial trace for a subsystem \bar{X} is carried out by the maximal depolarization channel [29] represented by an operator $|\rho\rangle\rangle$ [56],

which is given by

$$\hat{D}_{\bar{X}} = \prod_{j \in \bar{X}} \hat{D}_j^m, \quad (\text{A1})$$

$$\hat{D}_j^m = \frac{1}{4} \left[\hat{I}_{j,u} \otimes \hat{I}_{j,\ell} + \hat{X}_{j,u} \otimes \hat{X}_{j,\ell} - \hat{Y}_{j,u} \otimes \hat{Y}_{j,\ell} + \hat{Z}_{j,u} \otimes \hat{Z}_{j,\ell} \right], \quad (\text{A2})$$

where $\hat{I}_{j,u(\ell)}$ is an identity operator for site- j vector space in $\mathcal{H}_{u(\ell)}$, $\hat{Z}(X, Y)_{j,u(\ell)}$ is Pauli- $Z(X, Y)$ operator at site j . The channel operator $\hat{D}_{\bar{X}}$ is a coupling between the system u and ℓ in the ladder system. We apply $\hat{D}_{\bar{X}}$ to a state $|\rho\rangle\rangle$ [57]. Then, we obtain

$$\hat{D}_{\bar{X}}|\rho\rangle\rangle = |\frac{\mathbf{I}_{\bar{X}}}{d_{\bar{X}}} \otimes \rho_X\rangle\rangle, \quad (\text{A3})$$

where $d_{\bar{X}}$ is the number of degree of freedom of the subsystem \bar{X} and $|\frac{\mathbf{I}_{\bar{X}}}{d_{\bar{X}}} \otimes \rho_X\rangle\rangle \longleftrightarrow \frac{\mathbf{I}_{\bar{X}}}{d_{\bar{X}}} \otimes [\text{Tr}_{\bar{X}} \rho]$.

For the above vector, we consider the norm. Then, the norm of the state $\hat{D}_{\bar{X}}|\rho\rangle\rangle$ is related to $S_X^{(2)}$ as follows[58],

$$\langle\langle \frac{\mathbf{I}_{\bar{X}}}{d_{\bar{X}}} \otimes \rho_X | \frac{\mathbf{I}_{\bar{X}}}{d_{\bar{X}}} \otimes \rho_X \rangle\rangle = \frac{1}{d_{\bar{X}}} \text{Tr}_X [\rho_X^2]. \quad (\text{A4})$$

Thus, we obtain $S_X^{(2)}$ from $\hat{D}_{\bar{X}}|\rho\rangle\rangle$ as

$$S_X^{(2)} = -\log \left[d_{\bar{X}} \langle\langle \frac{\mathbf{I}_{\bar{X}}}{d_{\bar{X}}} \otimes \rho_X | \frac{\mathbf{I}_{\bar{X}}}{d_{\bar{X}}} \otimes \rho_X \rangle\rangle \right]. \quad (\text{A5})$$

The operation of Eq. (A3) and the norm calculation in Eq. (A4) can be performed by the MPS numerical-based filtering methods. Furthermore, we suitably set the subsystem X and take a suitable combination. Then we obtain the R2MI, $MI^{(2)}(L_A)$.

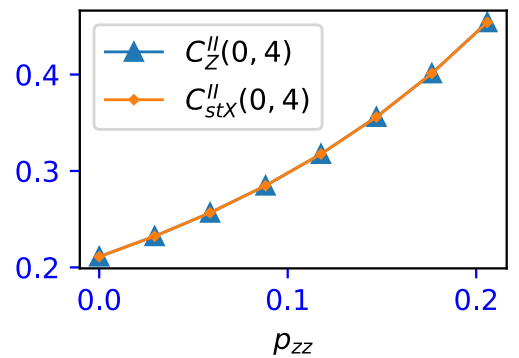


FIG. A1. Comparison between C_{ZZ}^{II} and C_{stX}^{II} . We set $J = h = 1$ and use $L = 28$ system.

Appendix B: Canonical two point correlator from the doubled Hilbert space formalism

For the 1D TFIM under the decoherence, the canonical two point correlator is given by $\text{Tr}[\rho_D Z_i Z_j]$. This observable is employed as an order parameter characterizing the ordinary long-range order. The expression in the doubled Hilbert space formalism is given by using the Choi isomorphism formula for a density matrix ρ [35, 37]. In general, the density matrix is represented by

$$|\rho\rangle\rangle = \frac{1}{\sqrt{\dim[\rho]}} \sum_k |k\rangle \otimes \rho|k\rangle,$$

where $\{|k\rangle\}$ is a basis set on the single \mathcal{H} . Here, we consider an infinite temperature state, $\rho = \hat{I}/2^L$. The state $\rho = \hat{I}/2^L$ can be regarded as a product state of the superposed triplet state with equal weight as shown in the main text, where we take the set of basis $\{|k\rangle\}$ as the spin z -component bases. Then, the canonical correlator $\text{Tr}[\rho_D Z_i Z_j]$ for a decohered

state ρ_D is expressed as

$$\text{Tr}[\rho_D Z_i Z_j] = \text{Tr}[\rho_D Z_i Z_j \hat{I}] = \frac{\langle\langle \mathbf{1} | Z_{i,u} Z_{j,u} | \rho_D \rangle\rangle}{\langle\langle \mathbf{1} | \rho_D \rangle\rangle}.$$

The above quantity is C_Z^I in the main text.

Appendix C: Confirmation of Krammers-Wannier duality in weak symmetry sense

We consider the KW transformed one of the $C_{ZZ}^{\text{II}}(0, r)$ given by

$$C_{stX}^{\text{II}}(0, r) = \text{Tr} \left[\left(\prod_{0 \leq \ell < r} X_\ell \right) \rho_D \left(\prod_{0 \leq \ell < r} X_\ell \right) \rho_D \right].$$

If the weak KW symmetry is sustained, then the equivalence, $C_{ZZ}^{\text{II}}(0, r) = C_{stX}^{\text{I}}(0, r)$ mentioned in the main text is expected.

Figure A1 is the numerical result for small p_{zz} regime, where we fix $r = 4$. We confirm that the equivalence is certainly satisfied. This means that the decoherence inherits the weakly symmetric KW dual and the decohered critical state is so.

-
- [1] C. W. Gardiner and P. Zoller, *Quantum Noise*, 2nd ed., edited by H. Haken (Springer, 2000).
 - [2] W. H. Zurek, *Decoherence and the transition from quantum to classical – revisited* (2003), [arXiv:quant-ph/0306072 \[quant-ph\]](#).
 - [3] J. Preskill, Quantum computing in the nisq era and beyond, *Quantum* **2**, 79 (2018).
 - [4] E. Dennis, A. Kitaev, A. Landahl, and J. Preskill, Topological quantum memory, *J. Math. Phys.* **43**, 4452–4505 (2002).
 - [5] C. Wang, J. Harrington, and J. Preskill, Confinement-higgs transition in a disordered gauge theory and the accuracy threshold for quantum memory, *Ann. Phys.* **303**, 31–58 (2003).
 - [6] T. Ohno, G. Arakawa, I. Ichinose, and T. Matsui, Phase structure of the random-plaquette z_2 gauge model: accuracy threshold for a toric quantum memory, *Nucl. Phys. B* **697**, 462 (2004).
 - [7] S. Ebadi, T. T. Wang, H. Levine, A. Keesling, G. Semeghini, A. Omran, D. Bluvstein, R. Samajdar, H. Pichler, W. W. Ho, S. Choi, S. Sachdev, M. Greiner, V. Vlatan, and M. D. Lukin, Quantum phases of matter on a 256-atom programmable quantum simulator, *Nature* **595**, 227 (2021).
 - [8] D. Bluvstein, S. J. Evered, A. A. Geim, S. H. Li, H. Zhou, T. Manovitz, S. Ebadi, M. Cain, M. Kalinowski, D. Hangleiter, J. P. Bonilla Ataides, N. Maskara, I. Cong, X. Gao, P. Sales Rodriguez, T. Karolyshyn, G. Semeghini, M. J. Gullans, M. Greiner, V. Vlatan, and M. D. Lukin, Logical quantum processor based on reconfigurable atom arrays, *Nature* **626**, 58 (2024).
 - [9] R. Fan, Y. Bao, E. Altman, and A. Vishwanath, Diagnostics of mixed-state topological order and breakdown of quantum memory, *PRX Quantum* **5**, 10.1103/prxquantum.5.020343 (2024).
 - [10] Z. Wang, Z. Wu, and Z. Wang, Intrinsic mixed-state topological order, *PRX Quantum* **6**, 010314 (2025).
 - [11] R. Sohal and A. Prem, Noisy approach to intrinsically mixed-state topological order, *PRX Quantum* **6**, 010313 (2025).
 - [12] Y. Kuno, T. Orito, and I. Ichinose, Intrinsic mixed-state topological order in a stabilizer system under stochastic decoherence: Strong-to-weak spontaneous symmetry breaking from a percolation point of view, *Phys. Rev. B* **111**, 064111 (2025).
 - [13] P. Di Francesco, P. Mathieu, and D. Sénéchal, *Conformal Field Theory*, Graduate texts in contemporary physics (Island Press, 1996).
 - [14] M. Henkel, *Conformal Invariance and Critical Phenomena*, Texts and monographs in physics (Springer, 1999).
 - [15] Y. Zou, S. Sang, and T. H. Hsieh, Channeling quantum criticality, *Phys. Rev. Lett.* **130**, 250403 (2023).
 - [16] Y. Kuno, T. Orito, and I. Ichinose, Rényi and shannon mutual information in critical and decohered critical system (2025), [arXiv:2506.18475 \[quant-ph\]](#).
 - [17] Y. Kuno, T. Orito, and I. Ichinose, System-environmental entanglement in critical spin systems under zz -decoherence and its relation to strong and weak symmetries (2025), [arXiv:2501.17481 \[quant-ph\]](#).
 - [18] M. Kohmoto, M. den Nijs, and L. P. Kadanoff, Hamiltonian studies of the $d = 2$ ashkin-teller model, *Phys. Rev. B* **24**, 5229 (1981).
 - [19] J. Sólyom, Duality of the block transformation and decimation for quantum spin systems, *Phys. Rev. B* **24**, 230 (1981).
 - [20] M. Yamanaka, Y. Hatsugai, and M. Kohmoto, Phase diagram of the ashkin-teller quantum spin chain, *Phys. Rev. B* **50**, 559 (1994).
 - [21] A. O’Brien, S. D. Bartlett, A. C. Doherty, and S. T. Flammia, Symmetry-respecting real-space renormalization for the quantum ashkin-teller model, *Phys. Rev. E* **92**, 042163 (2015).
 - [22] J. C. Bridgeman, A. O’Brien, S. D. Bartlett, and A. C. Doherty,

- Multiscale entanglement renormalization ansatz for spin chains with continuously varying criticality, *Phys. Rev. B* **91**, 165129 (2015).
- [23] P. Calabrese and J. Cardy, Entanglement entropy and quantum field theory, *J. Stat. Mech.* **2004**, P06002 (2004).
- [24] J.-M. Stéphan, G. Misguich, and V. Pasquier, Rényi entropy of a line in two-dimensional ising models, *Phys. Rev. B* **82**, 125455 (2010).
- [25] F. C. Alcaraz and M. A. Rajabpour, Universal behavior of the Shannon mutual information of critical quantum chains, *Phys. Rev. Lett.* **111**, 017201 (2013).
- [26] F. C. Alcaraz and M. A. Rajabpour, Universal behavior of the Shannon and Rényi mutual information of quantum critical chains, *Phys. Rev. B* **90**, 075132 (2014).
- [27] J.-M. Stéphan, Shannon and Rényi mutual information in quantum critical spin chains, *Phys. Rev. B* **90**, 045424 (2014).
- [28] T. Orito, Y. Kuno, and I. Ichinose, Strong and weak symmetries and their spontaneous symmetry breaking in mixed states emerging from the quantum ising model under multiple decoherence, *Phys. Rev. B* **111**, 054106 (2025).
- [29] M. A. Nielsen and I. L. Chuang, *Quantum Computation and Quantum Information*, 10th ed. (Cambridge University Press, USA, 2011).
- [30] Note that the order in application of the above local channels is irrelevant as long as we consider decoherence channels using Pauli operators such as $\mathcal{E}_{g_j}[\rho] = (1 - p)\rho + g_j \rho g_j^\dagger$, where g_j is an element of Pauli group with a finite length support. Then, general two channels are commutative, $\mathcal{E}_{g_j} \circ \mathcal{E}_{g_\ell}[\rho] = \mathcal{E}_{g_\ell} \circ \mathcal{E}_{g_j}[\rho]$ for either $[g_j, g_\ell] = 0$ or $\{g_j, g_\ell\} = 0$.
- [31] L. Li, M. Oshikawa, and Y. Zheng, Intrinsically/purely gapless-SPT from non-invertible duality transformations, *SciPost Phys.* **18**, 153 (2025).
- [32] C. de Groot, A. Turzillo, and N. Schuch, Symmetry protected topological order in open quantum systems, *Quantum* **6**, 856 (2022).
- [33] Y. Guo and Y. Ashida, Two-dimensional symmetry-protected topological phases and transitions in open quantum systems, *Phys. Rev. B* **109**, 195420 (2024).
- [34] J. Ashkin and E. Teller, Statistics of two-dimensional lattices with four components, *Phys. Rev.* **64**, 178 (1943).
- [35] M.-D. Choi, Completely positive linear maps on complex matrices, *Lin. Alg. Appl.* **10**, 285 (1975).
- [36] A. Jamiolkowski, Linear transformations which preserve trace and positive semidefiniteness of operators, *Rep. Math. Phys.* **3**, 275 (1972).
- [37] J. Y. Lee, C.-M. Jian, and C. Xu, Quantum criticality under decoherence or weak measurement, *Phys. Rev. X Quantum* **4**, 030317 (2023).
- [38] J. Y. Lee, Y.-Z. You, and C. Xu, Symmetry protected topological phases under decoherence, *Quantum* **9**, 1607 (2025).
- [39] The coefficient of the last line in Eq.(3) is given by $C(p_{zz}, p_x, L) \equiv (1 - 2p_{zz})^{L/2} (1 - 2p_x)^{L/2}$. The norm $\langle\langle \rho_D | \rho_D \rangle\rangle$ corresponds to the purity $\text{Tr}[\rho_D^2]$ (> 0), and the norm exhibits an exponential decay with the system size L due to the factor $C(p_{zz}, p_x, L)$.
- [40] E. Ardonne, P. Fendley, and E. Fradkin, Topological order and conformal quantum critical points, *Ann. Phys.* **310**, 493 (2004).
- [41] C. Castelnovo, C. Chamon, C. Mudry, and P. Pujol, From quantum mechanics to classical statistical physics: Generalized roksar–kivelson hamiltonians and the “stochastic matrix form” decomposition, *Ann. Phys.* **318**, 316–344 (2005).
- [42] C. Castelnovo and C. Chamon, Quantum topological phase transition at the microscopic level, *Phys. Rev. B* **77**, 054433 (2008).
- [43] J. Haegeman, K. Van Acoleyen, N. Schuch, J. I. Cirac, and F. Verstraete, Gauging quantum states: From global to local symmetries in many-body systems, *Phys. Rev. X* **5**, 011024 (2015).
- [44] G.-Y. Zhu and G.-M. Zhang, Gapless coulomb state emerging from a self-dual topological tensor-network state, *Phys. Rev. Lett.* **122**, 176401 (2019).
- [45] Y.-H. Chen and T. Grover, Unconventional topological mixed-state transition and critical phase induced by self-dual coherent errors, *Phys. Rev. B* **110**, 125152 (2024).
- [46] This effective Hamiltonian picture has succeeded in obtaining states close to the true ground states in various perturbed Hamiltonians such as Toric code [40–43].
- [47] P. Di Francesco, P. Mathieu, and D. Sénéchal, *Conformal field theory*, Graduate Texts in Contemporary Physics (Springer, Germany, 1997).
- [48] Y. Kuno, T. Orito, and I. Ichinose, Rényi markov length in one-dimensional non-trivial mixed state phases and mixed state phase transitions (2025), arXiv:2505.02125 [quant-ph].
- [49] L. A. Lessa, R. Ma, J.-H. Zhang, Z. Bi, M. Cheng, and C. Wang, Strong-to-weak spontaneous symmetry breaking in mixed quantum states, *PRX Quantum* **6**, 010344 (2025).
- [50] P. Sala, S. Gopalakrishnan, M. Oshikawa, and Y. You, Spontaneous strong symmetry breaking in open systems: Purification perspective, *Phys. Rev. B* **110**, 155150 (2024).
- [51] J. Hauschild and F. Pollmann, Efficient numerical simulations with Tensor Networks: Tensor Network Python (TeNPy), *SciPost Phys. Lect. Notes*, **5** (2018).
- [52] J. Hauschild, J. Unfried, S. Anand, B. Andrews, M. Bintz, U. Borla, S. Divic, M. Drescher, J. Geiger, M. Hefel, K. Hémerly, W. Kadow, J. Kemp, N. Kirchner, V. S. Liu, G. Möller, D. Parker, M. Rader, A. Romen, S. Scalet, L. Schoonderwoerd, M. Schulz, T. Soejima, P. Thoma, Y. Wu, P. Zechmann, L. Zweng, R. S. K. Mong, M. P. Zaletel, and F. Pollmann, Tensor network Python (TeNPy) version 1, *SciPost Phys. Codebases*, **41** (2024).
- [53] I. Affleck, Boundary condition changing operations in conformal field theory and condensed matter physics, *Nuclear Physics B - Proceedings Supplements* **58**, 35 (1997), proceedings of the European Research Conference in the Memory of Claude Itzykson.
- [54] N. Chepiga, Probing universal critical scaling with scan density matrix renormalization group, *Phys. Rev. B* **110**, 144401 (2024).
- [55] S. Sang and T. H. Hsieh, Stability of mixed-state quantum phases via finite markov length, *Phys. Rev. Lett.* **134**, 070403 (2025).
- [56] J. Y. Lee, Y.-Z. You, and C. Xu, Symmetry protected topological phases under decoherence, *Quantum* **9**, 1607 (2025).
- [57] Z. Zhang, Y. Zou, T. H. Hsieh, and S. Vijay, Universal properties of critical mixed states from measurement and feedback (2025), arXiv:2503.09597 [cond-mat.str-el].
- [58] R. Ma and A. Turzillo, Symmetry protected topological phases of mixed states in the doubled space (2024), arXiv:2403.13280 [quant-ph].